

---

## OMEGA Experimental Program and Recent Results

The Laboratory for Laser Energetics (LLE) with its OMEGA facility is part of the national laser-fusion effort within the U.S. Department of Energy and has as its main mission direct-drive laser-fusion research in support of the upcoming National Ignition Facility (NIF) at the Lawrence Livermore National Laboratory (LLNL). The upgraded OMEGA laser system has been in operation since May 1994. This versatile 60-beam UV laser facility has proven capable of carrying out a wide variety of experiments related to inertial confinement fusion (ICF). The facility also supports indirect-drive laser-fusion research under the direction of LLNL and the Los Alamos National Laboratory (LANL).

The challenges facing direct-drive ICF are principally connected with drive uniformity (uniformity of laser irradiation on target), control of the hydrodynamic instabilities during the compression phase of the target, and target uniformity, particularly that of the future cryogenic targets required for the success of laser fusion. The experimental program at LLE addresses all of these issues; this article lays out the present status of this research and its path for the future.

The *irradiation uniformity* on target depends on the number of laser beams and their disposition, the intensity distribution within each beam (beam-smoothing scheme), and the energy and instantaneous power of each beam (energy and power balance). While the first two points are unalterable characteristics of the OMEGA laser system (60 beams symmetrically disposed around the target), all other contributors to the irradiation nonuniformity are subject to ongoing research and improvements. The ultimate goals for OMEGA are 4%–5% rms beam-to-beam energy and power balance and <1% rms irradiation uniformity averaged over the target and over 300 to 500 ps.

*Understanding and controlling the hydrodynamic instabilities* are the main ICF concerns. Of primary concern is the Rayleigh–Taylor (RT) instability in the acceleration and deceleration phases of the spherically imploding ICF target. The problem centers on both growth rates and relevant seed amplitudes from which target perturbations can grow. LLE has

established experimental programs to address both issues. The seed amplitudes can be due to either laser nonuniformities (laser imprinting) or target nonuniformities. The role of drive-generated seed amplitudes (laser imprinting) is studied extensively at LLE. Assessment and improvements of target nonuniformities (particularly those of cryogenic targets) are addressed elsewhere within the national program. RT growth rates have been studied in a collaborative effort between LLNL and LLE for some time. The present LLE experimental program on RT growth rates addresses the problem in both planar and spherical geometries and for a variety of irradiation and laser-beam-smoothing techniques.

LLE is preparing for future cryogenic target irradiation through a program centered at General Atomic in San Diego. Cryogenic targets will be irradiated on OMEGA within two to three years.

### OMEGA Laser Characteristics

The OMEGA laser system<sup>1</sup> is a Nd:glass laser system with frequency conversion to the third harmonic with a UV (351-nm) energy capability on target in excess of 30 kJ for pulse durations of  $\leq 2$  ns. The system's 60 beams (30-cm beam diameter) are arrayed symmetrically around the 3.3-m-diam target chamber and are focused onto the target by 60 near-diffraction-limited  $f/6$  lenses.

Laser pulses with a wide variety of predetermined, temporal UV output pulse shapes have been produced by a versatile pulse-shaping system.<sup>2,3</sup> To date these shapes range from 1- to 3-ns flat-topped pulses to linear ramps (1 to 3 ns), Gaussians (0.2 to 1.2 ns), and LLNL's pulse shape PS22 (2-ns pulse designed for indirect-drive targets).

The demonstrated energy balance of the OMEGA system is ~2% rms for the IR part of the system, ~3% rms in the UV after the conversion crystals, and ~4% to 5% rms on target after the UV transport optics (two turning mirrors, a focusing lens, and a blast shield per beamline). The system's energy reproducibility is <1% rms excluding clearly identifiable flashlamp or

pulse-forming network (PFN) malfunctions. The measurement accuracy of the beam energies (including residual fundamental and second-harmonic output from the conversion crystals) is  $\sim 0.8\%$  rms.

The laser system has three complete driver lines with corresponding pulse-shaping systems. Any one or any combination of two of these driver lines can be used to drive the laser system. The laser system supports the propagation of two different pulse shapes, one for the main experiment (driver) and one for a backlighter. In this case one driver line feeds 40 beamlines, while the other feeds the remaining 20. The timing between these two groups of beams can be chosen freely.

Beam smoothing—an essential component for the success of direct-drive laser fusion—is implemented on OMEGA using smoothing by spectral dispersion (SSD) pioneered at LLE.<sup>4</sup> LLE's approach combines continuous-phase-plate technology with polarization rotators and two frequency modulators with corresponding spectral dispersion in two dimensions (2-D SSD). Present capabilities are limited to 2- to 3-Å total bandwidth for the two modulators (3- and 3.3-GHz modulation frequency). In addition, a limited number of phase plates and polarization rotators are available primarily for planar-target experiments. By the end of 1997 a full complement of phase plates will be available for spherical irradiation experiments. A complete complement of polarization rotators is projected for 1 to 2 years from now. At that time increased bandwidth ( $\sim 10$  Å) and frequency modulation (FM) at higher frequencies ( $\sim 10$  GHz) will also be available, allowing an on-target frequency bandwidth of  $\sim 1$  THz in the UV.

The pointing capability of the OMEGA laser system has been shown to be  $\sim 10$   $\mu\text{m}$  rms on target. This performance has been repeatedly verified with x-ray imaging using pinhole cameras and x-ray microscopes. The stability of the system is sufficient to maintain the above pointing accuracy without adjustments for at least a period of one day. Furthermore, recent experiments have shown that beams can be placed in basically arbitrary locations within  $\sim 1$  cm from the target chamber center with essentially the same accuracy ( $\sim 20$   $\mu\text{m}$  without corrections; better accuracy is achievable with one iterative fine correction). This capability has been demonstrated on recent indirect-drive hohlraums of cylindrical (two laser entrance holes) and spherical shape (“tetrahedral” hohlraums with four laser entrance holes) with or without additional backlighter targets.

## Present OMEGA Experiments

The present OMEGA experiments address irradiation uniformity, implosion physics, hydrodynamic instabilities, laser imprinting, and laser–plasma–interaction physics. In addition LLNL and LANL carry out experiments related to indirect-drive laser fusion.

### 1. Irradiation Uniformity

The irradiation uniformity on target can be analyzed using spherical harmonic decomposition. One thus finds that the unalterable OMEGA irradiation configuration (60 beams symmetrically arrayed around the target) and the on-target beam envelopes contribute primarily to modes of order  $\ell < 20$ . Energy and power balance as well as pointing on target contribute predominately to the amplitudes of modes with  $\ell \leq 4$ . The intensity distributions of the individual beams, on the other hand, contribute to high-order modes with  $\ell$  ranging well beyond  $\ell = 100$ . The effort to control and reduce the irradiation uniformity on target therefore requires many different approaches.

a. Energy and power balance. Energy and power balance of  $\sim 4\%$ – $5\%$  rms between beams puts severe demands on the laser system. Very accurate energy- and pulse-shape-measurement capabilities are a prerequisite, as are stringent controls over the gains and losses of like amplification stages within the system (they must be kept within  $\sim 2\%$  rms). In addition, computer-based strategies must be developed for energy redistribution and fine control of some key amplifiers.

The energy-measurement requirements have been met by OMEGA. The capability to sufficiently control the individual beam energies has also been demonstrated; however, some persistent problems with PFN's presently prevent consistent achievement of the desired and achievable energy balance of  $\leq 4\%$  rms on target. This goal will only be achieved after some critical components that currently perform marginally are replaced.

Power balance on OMEGA has so far been addressed primarily conceptually. Some significant improvements in pulse-shape-measurement capability will result when two high-quality multiplexed UV streak cameras are installed on OMEGA within the next two to three months. They will measure the pulse shapes of 20 of the 60 OMEGA beams. The expected measurement accuracy is  $\sim 1\%$  rms at the peak of the pulse for all 20 channels with an optical fiducial channel providing

timing accuracy and on-shot sweep speed calibration. (In addition, a new streak camera tube, designed at LLE and built by Phillips in France, is expected to provide a higher dynamic range and more extended multiplexing capabilities.)

An essential component of LLE's power balance strategy relies on the fact that power balance is assured if energy balance is maintained for full-energy shots as well as for shots with reduced output energy. Of course, the laser system must be operated under identical conditions (e.g., identical bank voltages) with only the input laser energy reduced appropriately.

**b. Beam-intensity distribution and smoothing mechanisms.**

The intensity distribution of a typical high-power laser beam on target is shown in Fig. 72.1(a). The target outline is indicated by the circle. The introduction of a distributed (quasi-random) phase plate (DPP) with continuous phase relief generates an intensity distribution [Fig. 72.1(b)] whose envelope and speckle pattern are statistically well defined. In addition, LLE's phase-plate approach allows for control of both the envelop function and the speckle distribution. SSD combines FM with spectral dispersion to smooth the high-frequency speckle of the DPP's leading to the very smooth intensity distribution shown in Fig. 72.1(c). This figure is a temporal average over the full pulse duration of 1 ns. Instantaneously, the intensity distribution is still as shown in Fig. 72.1(b).

Further enhancement of the uniformity (smoothness) of the single-beam-intensity distribution on target is obtained by using polarization rotators.<sup>5</sup> These optics are birefringent wedges that are placed in the beam near the focusing lens and change the polarization across the beam in a continuous manner. The effect of this plate is equivalent to splitting the beam into two orthogonal polarization components whose indepen-

dent speckle patterns on target are slightly displaced and do not interfere with each other. This leads to an instantaneous reduction in beam nonuniformity by a factor of  $\sqrt{2}$ . LLE is currently developing liquid crystal polarization rotators for all 60 beams of OMEGA.

**2. Implosion Physics**

Implosion experiments have been conducted on the upgraded OMEGA since it was commissioned in May 1994. The improved symmetry of irradiation and the 30-kJ energy capability of this laser system immediately resulted in record neutron yields in excess of  $10^{14}$  for ~30-kJ UV irradiation of a DT-filled glass shell of ~1-mm diameter.

A series of recent implosion experiments were designed to investigate the scaling of the measured neutron yields with expected core distortions due to the combined effects of the RT instability in the ablation and deceleration phases. For this purpose, targets with different fill pressures and various shell compositions (CH and Cl-doped CH shells) were used. A corresponding plot is shown in Fig. 72.2, where the relative neutron yield is plotted as a function of the expected distortion fraction of the fully imploded target. The distortion fraction was obtained from ancillary calculations using current models for the RT growth factor in the acceleration (ablation) phase, a heuristic feedthrough factor for the perturbations from the outer to the inner pusher surfaces, and similar RT growth factor estimates for the deceleration phase. This distortion fraction is the radial core distortion divided by the final radius of the imploded core. The smooth scaling of these data for a variety of targets and irradiation conditions suggests that this definition of the distortion fraction of the final core is a useful one, combining RT instability and target convergence concepts.

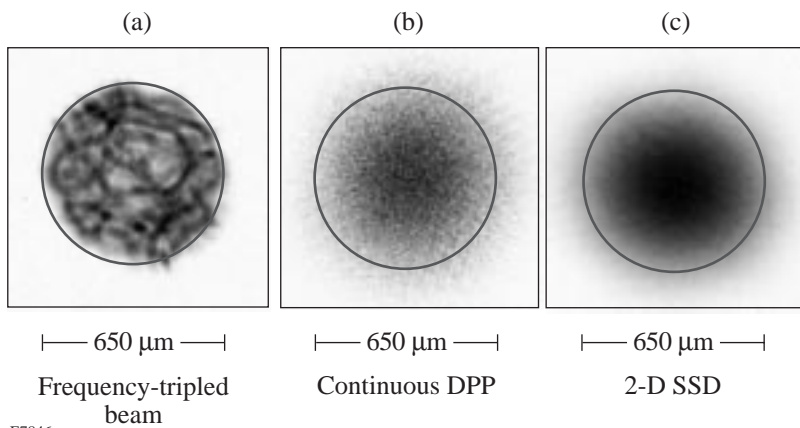


Figure 72.1  
The intensity distribution of a single beam in the target plane for (a) a typical high-power laser beam without any smoothing, (b) the same beam as modified (aberrated) by a phase plate with a continuous-phase-relief pattern, and (c) 2-D SSD (phase plate and two FM modulators with wavelength dispersion in two perpendicular directions).

E7846

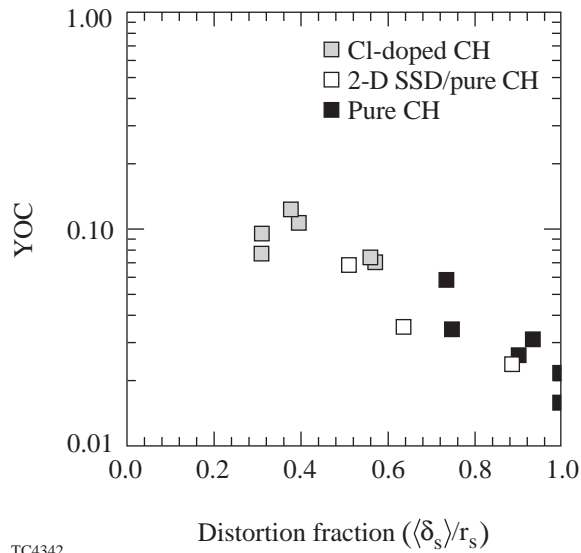


Figure 72.2

The yield over calculated 1-D yield (YOC) scales reproducibly with the distortion fraction, which is defined as the distortion of the final core relative to its radius. This distortion fraction is obtained from ancillary calculations using models for the RT growth factors in the ablation (acceleration) phase, a heuristic feedthrough factor, and the growth factor of the deceleration phase.

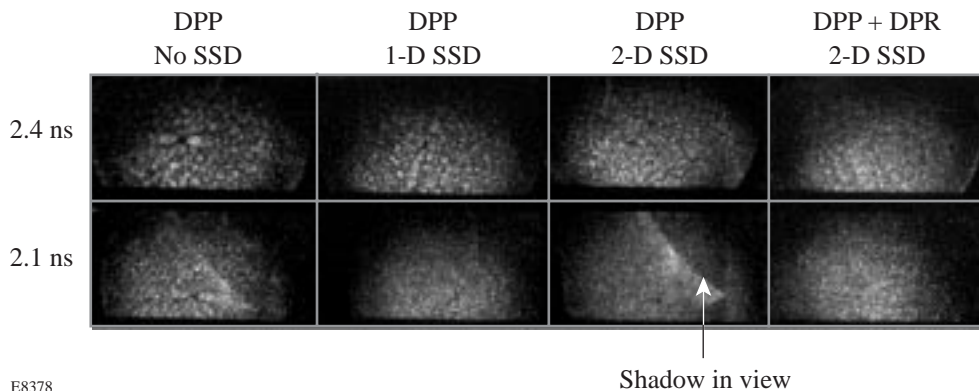
Several experimental programs at LLE investigate various aspects of the RT instability: two planar-foil experiments study laser imprinting and RT growth rates respectively, and several spherical target experiments address RT growth in both the ablation and deceleration phases.

**a. Laser imprinting (planar targets).** Laser imprinting has been studied at LLE using planar foils and multiple-beam irradiation (typically five to six overlapping beams). The experimental variables included various beam-smoothing techniques and foam-coated targets. Face-on radiography (85-ps exposure time) was used to measure the modulation depth as a function of time (Fig. 72.3). Initial mass perturbations caused by laser imprinting are amplified by the subsequent RT growth and are observed later in time. In other words, the mass perturbations that are initially invisible are rendered visible by the RT amplifier. Changing the smoothness of the laser irradiation (from no DPP's to DPP with 1-D SSD, etc.) one clearly discerns a corresponding decrease in modulation depth at late times. Full 2-D SSD with distributed polarization rotators (DPR's) leads to greatly reduced modulation, indicating significantly reduced laser imprinting. Fourier analysis of the images in Fig. 72.3 also shows clear quantitative reduction in the power spectrum for spatial wavelengths in the range of 20 to 100  $\mu\text{m}$ .<sup>6</sup>

TC4342

### 3. Hydrodynamic Instabilities

The hydrodynamic instabilities encountered in direct-drive ICF are generally dominated by the RT instability. This instability is active during the target implosion in both the acceleration phase at the ablation interface and the deceleration phase at the fuel–pusher interface before the final stagnation. The instability grows from target imperfections and/or mass perturbations produced by irradiation nonuniformities (laser imprinting). This laser imprinting occurs primarily at early times when there is little or no plasma to smooth irradiation nonuniformities. Since some degree of irradiation nonuniformity is unavoidable, a thorough understanding of the RT growth rates is vital, particularly with regard to effects that may reduce the growth rates.



E8378

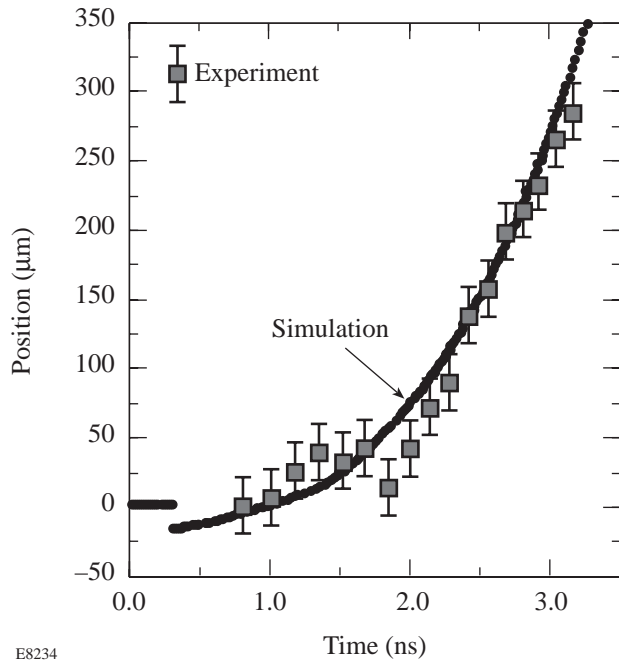
Figure 72.3

Laser imprinting using planar foils and five overlapping beams (3 ns flat-top) clearly shows the effect of different smoothing techniques applied to the laser beam. The modulation face-on radiographs taken in the light of an x-ray backlighter around 2 keV are less pronounced at early times than later (2.1 ns versus 2.4 ns) when RT growth of the laser imprint becomes much more noticeable.

Foam-covered targets have been proposed to decrease laser imprinting as well as reduce RT growth rates.<sup>7</sup> Imprint experiments using such foam-covered targets do indeed exhibit significantly reduced laser imprinting, but the analysis of these experiments is rendered more complex due to possible changes in target isentrope, which can reduce the RT growth rates. To assess the utility of foam-covered targets all effects on target dynamics must be considered.

**b. RT growth (planar target).** Detailed studies of the RT growth rates in direct-drive experiments have been carried out for some time in collaboration with LLNL.<sup>8</sup> These experiments were initiated on the Nova laser at LLNL and were subsequently moved to OMEGA.<sup>9</sup> The generic setup for these experiments utilized flat-foil targets with known mass perturbations that were irradiated with five or six overlapping drive beams. These drive beams were outfitted with DPP's and other variants of beam smoothing. The targets were radiographed with an x-ray backlighter and an x-ray framing camera. In addition, acceleration measurements of the foil were taken with a streak camera and side-on x-ray backlighting.

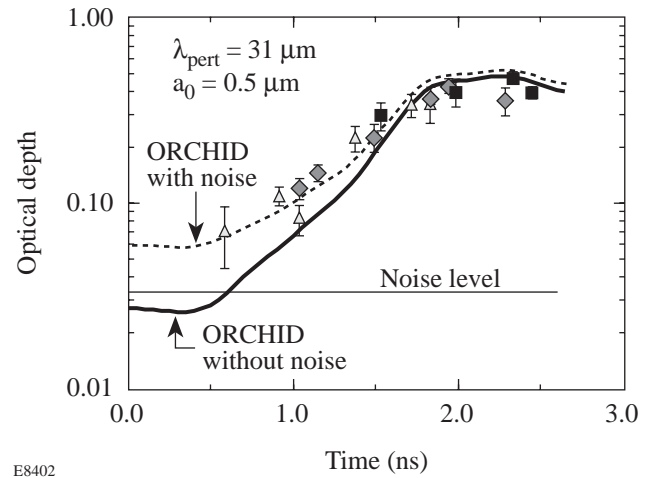
Quantitative interpretation of the RT growth rates requires accurate knowledge of the laser coupling to, and the resulting



E8234  
 Figure 72.4  
 Trajectory of accelerated 20- $\mu\text{m}$  CH foil targets used for RT experiments. The experimental data were obtained using an x-ray streak camera with side-on backlighting of the planar-foil target. The solid line corresponds to numerical predictions using the experimental laser pulse shapes.

acceleration of, this target. Furthermore, since all RT growth rate interpretation requires code simulations, a prerequisite for success is good agreement between the time history of the accelerated target position and code predictions. Such agreement is shown in Fig. 72.4 for a bare (smooth) 20- $\mu\text{m}$  CH target foil accelerated by a 3-ns ramp laser pulse. Similar experiments using foam-covered targets yielded equally good results and indicated unchanged coupling of the laser to the target.<sup>9</sup>

The RT growth of single-frequency sinusoidal perturbations impressed on the target has been measured using initial perturbation amplitudes of  $\sim 0.5\text{-}\mu\text{m}$  with 31- $\mu\text{m}$  and 60- $\mu\text{m}$  wavelengths. Initially these perturbations are invisible in the framing images of the backlit foil, but at later times the perturbations become clearly visible and measurable. Plotting the optical depth versus time (Fig. 72.5) shows the expected signature of RT growth. Since the optical-depth fluctuations are proportional to areal density ( $\rho r$ ) changes along the line of sight, one interprets modulation fluctuations as perturbation amplitudes assuming constant density  $\rho$ . In order to extract quantitative information from this plot, numerical simulations are carried out using the 2-D hydrodynamic code *ORCHID*. Good agreement between these simulations and the experimental data in Fig. 72.5 is obtained provided the simulations use measured laser pulse shapes *and* include the experimentally measured noise in the x-ray framing camera snapshots. If



E8402  
 Figure 72.5  
 Rayleigh–Taylor growth as measured by the optical depth ( $\sim \rho r$  of the target) for a 20- $\mu\text{m}$ -thick CH foil with an impressed sinusoidal corrugation of 31- $\mu\text{m}$  wavelength and 0.5- $\mu\text{m}$  amplitude. The perturbation amplitude onset and saturation are well modeled by *ORCHID* simulations, provided the experimental noise in the framing-camera images is included in the analysis (dashed line).

the experimental noise were neglected, one might infer reduced (and erroneous) RT growth rates. Furthermore, proper interpretation of RT experiments requires allowance for nonconstant target acceleration and the concomitant change in RT growth rates.

**c. Ablative RT instability in spherical targets.** Burnthrough experiments using imploding spherical targets with high-Z signature layers have been carried out at LLE for approximately five years.<sup>10</sup> These experiments have clearly shown that the measured time of appearance of the x-ray lines due to the signature layer is more indicative of the RT instability in the ablation phase than of the propagation of the ablation front. Recent experiments on OMEGA have confirmed the earlier observations and refined the interpretation in terms of equivalent initial mass perturbations, which may be due to laser imprinting or target nonuniformities. Changing beam smoothing permits quantitative estimates for the laser imprinting in terms of equivalent target nonuniformities.

**d. Deceleration-phase RT instability (mixing).** The RT instability during the final stages of the implosion (the deceleration phase) has been investigated at LLE using various signature layers close to the inner boundaries of the target.<sup>11,12</sup> These layers are either Ti-doped plastic layers with a 10- to 20- $\mu\text{m}$  CH ablation layer on the outside or 2- $\mu\text{m}$  CD layers similarly overcoated with an ablation layer. Between the signature layer and the inner target surface are CH layers of variable thickness. The target fill is either H<sub>2</sub>-Ar or D<sub>2</sub>-Ar for the two types of targets, respectively. The performance of these targets may be analyzed by using their neutron yield as a function of the innermost layer thickness or by x-ray spectroscopic means. These experiments are still in progress, and results indicate that this will be a powerful experimental technique.

#### 4. Laser–Plasma-Interaction Physics

A new series of laser–plasma-interaction physics experiments have recently been initiated at LLE. The first results pertain to scattering near the incident laser wavelength where stimulated Brillouin scattering (SBS) may be expected. Under current OMEGA irradiation conditions for spherical targets, 5% to 10% of the incident laser light is isotropically scattered due to refraction of the 60 OMEGA beams. The evolving plasma corona of the imploding targets imparts considerable bandwidth to this scattered light, which, however, bears no relationship to SBS. On the other hand, clear signatures of SBS have been observed in implosion experiments when one beam was focused to  $\sim 10^{15}$  W/cm<sup>2</sup> ( $R_{\text{SBS}} \approx 12\%$ ).

The presence of a vigorously excited two-plasmon-decay instability is clearly seen in all implosion experiments on OMEGA. This instability has an experimental threshold in the low  $10^{13}$  W/cm<sup>2</sup> and is difficult to suppress with any beam-smoothing techniques.<sup>13</sup> The importance of this instability lies in its potential to generate energetic electrons. We are presently preparing to quantify any energetic electron production that may accompany this instability.

In the spectral region where one expects to observe stimulated Raman scattering (480 to 700 nm), we have observed scattering in a number of implosion experiments. However, indications are that this instability is close to its threshold under typical OMEGA operating conditions (a few  $10^{14}$  W/cm<sup>2</sup>).

Long-scale-length experiments have begun using exploding foil or solid targets with multiple-beam irradiation and staggered timing of the various beam clusters. These experiments are guided by 2-D hydrodynamic (*SAGE*) simulations that predict  $\sim 1$ -mm density-gradient lengths at  $n_c/8$  at electron temperatures in excess of 2 keV.

#### Summary

The 60-beam OMEGA laser system has now been in operation for three years. It has been used extensively for a wide variety of experiments relating to direct-drive laser fusion, from high-yield implosion experiments to planar and spherical Rayleigh–Taylor experiments and laser-imprinting experiments as well as laser–plasma-interaction experiments. OMEGA is a versatile and effective target irradiation facility that will support the National Ignition Facility now under construction at LLNL. Experimental results obtained to date pertain to both direct-drive and indirect-drive laser fusion.

#### ACKNOWLEDGMENT

This work was supported by the U.S. Department of Energy Office of Inertial Confinement Fusion under Cooperative Agreement No. DE-FC03-92SF19460, the University of Rochester, and the New York State Energy Research and Development Authority. The support of DOE does not constitute an endorsement by DOE of the views expressed in this article.

#### REFERENCES

1. T. R. Boehly, R. S. Craxton, R. J. Hutchison, J. H. Kelly, T. J. Kessler, S. A. Kumpan, S. A. Letzring, R. L. McCrory, S. F. B. Morse, W. Seka, S. Skupsky, J. M. Soures, and C. P. Verdon, in *Solid State Lasers III*, edited by G. J. Quarles (SPIE, Bellingham, WA, 1992), Vol. 1627, pp. 236–245.
2. R. L. Keck, A. V. Okishev, M. D. Skeldon, A. Babushkin, and W. Seka, “Pulse Shaping on the OMEGA Laser System,” to be published in the

- Proceedings of the Thirteenth International Conference on Laser Interactions and Related Plasma Phenomena (LIRPP)*, Monterey, CA, 13–18 April 1997.
3. A. Okishev, M. D. Skeldon, S. A. Letzring, W. R. Donaldson, A. Babushkin, and W. Seka, in *Superintense Laser Fields*, edited by A. A. Andreev and V. M. Gordienko (SPIE, Bellingham, WA, 1996), Vol. 2770, pp. 10–17.
  4. S. Skupsky, R. W. Short, T. Kessler, R. S. Craxton, S. Letzring, and J. M. Soures, *J. Appl. Phys.* **66**, 3456 (1989).
  5. T. E. Gunderman, J.-C. Lee, T. J. Kessler, S. D. Jacobs, D. J. Smith, and S. Skupsky, in *Conference on Lasers and Electro-Optics*, Vol. 7, 1990 OSA Technical Digest Series (Optical Society of America, Washington, DC, 1990), p. 354.
  6. T. R. Boehly, D. D. Meyerhofer, J. P. Knauer, D. K. Bradley, R. L. Keck, V. A. Smalyuk, W. Seka, and C. P. Verdon, “Laser-Imprinting Studies on the OMEGA Laser System,” to be published in the *Proceedings of the Thirteenth International Conference on Laser Interactions and Related Plasma Phenomena (LIRPP)*, Monterey, CA, 13–18 April 1997.
  7. M. Desselberger *et al.* *Phys. Rev. Lett.* **74**, 2961 (1995).
  8. S. G. Glendinning, S. V. Weber, P. Bell, L. B. DaSilva, S. N. Dixit, M. A. Henesian, D. R. Kania, J. D. Kilkenny, H. T. Powell, R. J. Wallace, P. J. Wegner, J. P. Knauer, and C. P. Verdon, *Phys. Rev. Lett.* **69**, 1201 (1992).
  9. J. P. Knauer, D. D. Meyerhofer, T. R. Boehly, D. Ofer, C. P. Verdon, D. K. Bradley, P. W. McKenty, V. A. Smalyuk, S. G. Glendinning, and R. G. Watt, “Single-Mode Rayleigh–Taylor Growth-Rate Measurements with the OMEGA Laser System,” to be published in the *Proceedings of the Thirteenth International Conference on Laser Interactions and Related Plasma Phenomena (LIRPP)*, Monterey, CA, 13–18 April 1997.
  10. J. Delettrez, D. K. Bradley, and C. P. Verdon, *Phys. Plasmas* **1**, 2342 (1994).
  11. B. Yaakobi, F. J. Marshall, D. K. Bradley, J. A. Delettrez, R. S. Craxton, and R. Epstein, *Phys. Plasmas* **4**, 3021 (1997).
  12. Laboratory for Laser Energetics LLE Review **70**, 82, NTIS document No. DOE/SF/19460-164 (1997). Copies may be obtained from the National Technical Information Service, Springfield, VA 22161.
  13. W. Seka, R. E. Bahr, R. W. Short, A. Simon, R. S. Craxton, D. S. Montgomery, and A. E. Rubenchik, *Phys. Fluids B* **4**, 2232 (1992).